

Inferring taxonomic placement from DNA barcoding allowing discovery of new taxa

Alessandro Zito¹, Tommaso Rigon², and David B. Dunson¹

¹Department of Statistical Science, Duke University, Durham, NC, 27708, U.S.A.

²Department of Economics, Management and Statistics, University of Milano-Bicocca, Milan, 20126, Italy

Abstract

In ecology it has become common to apply DNA barcoding to biological samples leading to datasets containing a large number of nucleotide sequences. The focus is then on inferring the taxonomic placement of each of these sequences by leveraging on existing databases containing reference sequences having known taxa. This is highly challenging because i) sequencing is typically only available for a relatively small region of the genome due to cost considerations; ii) many of the sequences are from organisms that are either unknown to science or for which there are no reference sequences available. These issues can lead to substantial classification uncertainty, particularly in inferring new taxa. To address these challenges, we propose a new class of Bayesian nonparametric taxonomic classifiers, BayesANT, which use species sampling model priors to allow new taxa to be discovered at each taxonomic rank. Using a simple product multinomial likelihood with conjugate Dirichlet priors at the lowest rank, a highly efficient algorithm is developed to provide a probabilistic prediction of the taxa placement of each sequence at each rank. BayesANT is shown to have excellent performance in real data, including when many sequences in the test set belong to taxa unobserved in training.

1 INTRODUCTION

DNA barcoding refers to the practice of identifying the taxonomic affiliation of unknown specimens through short fragments of their DNA molecular sequence called barcoding genes. Typically, this assessment is performed by comparing the DNA obtained from the high-throughput sequencing of a bulk sample to a library of genes whose Linnean taxonomy is well-established. Examples of these collections are numerous, with the Barcode of Life project ([Sarkar and Trizna, 2011](#)) being a particularly notable case. In order for the identification to be reliable, reference DNA sequences should be

characterized by limited intra-species and high inter-species gene variation, and should be sufficiently simple to align and compare (Hebert et al., 2003). In the animal kingdom and in insects especially, these characteristics have been found in a region of approximately 650-base-pairs near the 5th end of the mitochondrial cytochrome c oxidase sub-unit I, or COI, gene (Janzen et al., 2005). This region has become routinely used in animal species identification. In particular, libraries are formed by clustering similar COI sequences under a common Barcode Index Number, or BIN, which identifies a given species (Ratnasingham and Hebert, 2013).

The impact of DNA barcoding in biodiversity assessment has been dramatic. It took more than 200 years to describe approximately 1 million species of insects through morphological inspection, whereas nearly 400,000 BINs have been categorized within the span of just 10 years (Wilson et al., 2017). DNA barcoding offers a way to categorize the large quantities of specimens collected by modern automatic sampling methods. For example, flying insects are routinely captured with Malaise traps (Malaise, 1937), which collect the sampled insects together in a ‘soup’ within a storage cylinder. While this method often causes deterioration of the captured animals, making them morphologically unrecognizable, the biologic material in the soup can be processed relatively cheaply (Shokralla et al., 2014) and later used for identification. The practice of DNA sequencing from a bulk sample is known as DNA metabarcoding (Yu et al., 2012). The output of a metabarcoding procedure is the grouping of similar sequences detected in the samples into *operational taxonomic units*, or OTUs. These OTUs provide initial hypothesized species labels for the animals in the sample, and assessing their taxonomic placement is the final key stage of a bioinformatics pipeline.

Despite the advantages described above, taxonomic assessment of OTUs presents its own challenges, especially at lower level ranks. While it is relatively easy to accurately place a DNA sequence to a *Phylum*, a *Class* or an *Order* (Yu et al., 2012), the information obtainable via high-throughput methods is limited by the short length of the sequences extracted. This makes the identification at the *Family*, at the *Genus* and at the *Species* level subject to higher uncertainty (Pentinsaari et al., 2020). Moreover, DNA metabarcoding may be prone to sequencing and clustering errors. As a consequence, it can either split biologic material from the same species into two different clusters, or merge different species into a single cluster (Somervuo et al., 2017). Finally, reference sequence libraries can be subject to mislabelling errors (Somervuo et al., 2016) and are necessarily incomplete. This leads to the necessity of developing classification methods that provide a reliable characterization of uncertainty in assigning the taxa of the collected OTUs, accounting for the possibility that they might identify a new species or one for which information is not available. Such methodologies allow one to quantify the biodiversity of a given sampling region, which is an urgent problem considering the recent evidence of insect biomass decline (Seibold et al., 2019).

Various software for taxonomic recognition have been developed, relying on different prediction methods. One approach labels a query DNA with the taxon of the reference sequence having the highest similarity (Huson et al., 2007; Nguyen et al., 2014). This requires applying local or global alignment procedures to the sequences in the library, such as the BLAST - Basic Local Alignment Search Tool - similarity score (Altschul et al., 1990). When alignment is undesirable due to computational costs, fast algorithms that exploit a κ -mer representation of the sequences can be adopted. Widely used examples are the Naïve Bayes RDP classifier (Wang et al., 2007) and its non-Bayesian heuristic alternatives (e.g SINTAX, Edgar, 2013). More recent methods use modern Machine Learning and Deep Learning techniques, such as Convolutional Neural Networks (Vu et al., 2020).

While these approaches can provide good classification results when the training data are sufficiently informative of the biodiversity of the environmental sample (Bazin et al., 2012), they can lead to unreliable matches when the reference sequence set is incomplete. Indeed, algorithms often do not account for unobserved taxa in a coherent way (Somervuo et al., 2017). One solution is to select a confidence probability cutoff, typically around 0.8, and regard the classification as unreliable if the predicted taxon has a probability below that threshold (Wang et al., 2007; Lan et al., 2012). Another alternative is to explicitly allow the algorithm to predict “new” taxa, as is done by PROTAX - PRObabilistic TAXonomic placement (Somervuo et al., 2016). PROTAX classifies DNA sequences by training a multinomial regression model on a subsample of the reference library reflecting prior knowledge on the existing taxonomy. The algorithm can lead to over- or under-detection of new species if the training dataset is not representative.

In this paper, we develop an off-the-shelf Bayesian nonparametric model for DNA barcoding that accounts for undetected nodes at every taxonomic rank. As our application mostly focuses on insects, we name our method BayesANT, short for BAYESiAn Nonparametric Taxonomic classifier. BayesANT computes taxon probabilities by combining a prior distribution for the taxonomic tree with a kernel-based approach to modelling the distribution of the nucleotide sequences linked to that taxon at the lowest rank. To obtain the prior, a Pitman–Yor process (Perman et al., 1992) is used to induce a species sampling model urn scheme (Blackwell and MacQueen, 1973; Pitman, 1996), which automatically specifies probabilities for the appearance of undiscovered species (Lijoi et al., 2007; Favaro et al., 2009; Zito et al., 2020) in a coherent way. For aligned sequences, we use a Dirichlet-multinomial product kernel over nucleotides, while, for unaligned sequences, we use a multinomial kernel over κ -mer counts. The resulting model facilitates fast computation of a probabilistic classifier, which provides careful uncertainty assessments in taxonomic annotations. We test BayesANT on a library of arthropod DNA sequences collected in Finland (Roslin et al., 2022). Technical and algorithmic details for BayesANT are reported in the Materials and Methods section, with further information in the Supplementary material.

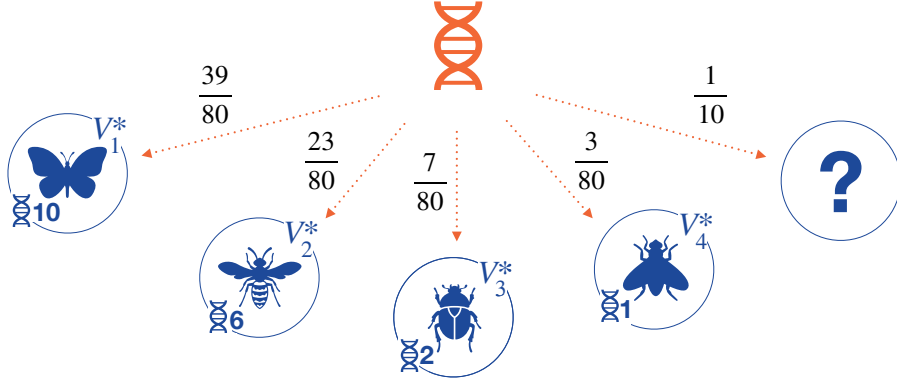


Figure 1: Example of a Pitman–Yor process with $n = 19$, $\alpha = 1$, $\sigma = 0.25$ and $K_n = 4$. Taxa names are reported on top of the circles, and frequencies of appearance are written on the right to the blue DNA sequences, respectively. Fractions in black denote the taxon probabilities for the orange DNA sequence. For example, the probability of observing the butterfly-shaped taxon V_1^* is $(n_1 - \sigma)/(\alpha + n) = (10 - 0.25)/(19 + 1) = 39/80$. The probability for the unknown question mark taxon is $(\alpha + \sigma k)/(\alpha + n) = (1 + 4 \times 0.25)/(19 + 1) = 1/10$.

2 PRELIMINARIES: THE PITMAN–YOR PROCESS

The Pitman–Yor ([Perman et al., 1992](#)) is a sequential process for label assignment whose allocation probabilities depend on two parameters, called α and σ , and on the size of the clusters previously detected. The allocation rule works as follows. Suppose that V_1, \dots, V_n are the taxon assignments for the DNA sequences in our library of barcodes at a given rank (such as *Phylum* or *Class*). Specifically, these sequences identify $K_n = k$ distinct taxa, named V_1^*, \dots, V_k^* , with frequencies n_1, \dots, n_k and $\sum_{j=1}^k n_j = n$. Then, the probability that the $(n + 1)$ st sequence belongs to the j th of the known taxa is

$$\text{pr}(V_{n+1} = V_j^* \mid V_1, \dots, V_n) = \frac{n_j - \sigma}{\alpha + n}, \quad (1)$$

for $j = 1, \dots, k$, while the probability of observing a new taxon is

$$\text{pr}(V_{n+1} = \text{“new”} \mid V_1, \dots, V_n) = \frac{\alpha + \sigma k}{\alpha + n}, \quad (2)$$

where $\alpha > -\sigma$ and $\sigma \in [0, 1)$. Figure 1 sketches the mechanism when $n = 19$ sequences and $k = 4$ different groups are observed. High values of α or values of σ close to 1 lead to a high probability of discovering a new taxon. The probability that a sequence is assigned to taxon label V_j^* increases with its abundance n_j . This process allows OTUs to be clustered together, through being assigned to the same existing or newly detected taxa. For further details, see ([Pitman, 1996](#); [De Blasi et al., 2015](#)).

3 CASE STUDY: THE FINNISH BARCODE OF LIFE LIBRARY

3.1 THE FINBOL LIBRARY

The Finland Barcode of Life initiative¹ (FinBOL) is a DNA barcoding library that contains reference sequences with highly reliable taxonomic annotations for the arthropod species of Finland. The data have been constructed placing substantial effort on barcode quality thanks to the collective effort of about 150 taxonomists. For a thorough description of how the library was assembled and later tested refer to Roslin et al. (2022).

The version of the data we consider contain a total of 34,624 DNA sequences annotated across 7 taxonomic levels, namely *Class*, *Order*, *Family*, *Subfamily*, *Tribe*, *Genus* and *Species*. Reference annotations are based off of the national checklist of Finnish species (FinBIF, 2020) with the inclusion of dummy taxa whenever *Subfamily* and *Tribe* were missing. The library has been globally aligned via Hidden Markov Models using the HMMER software (Eddy, 1995). As a result, each sequence has a length of 658 base pairs, consisting of nucleotides “A”, “C”, “G” and “T” and alignment gaps “-”. Other special characters are ignored and substituted with a gap for simplicity. Taxonomic labels in the data comprise 3 *Classes*: *Arachnida*, *Insecta* and *Malacostraca*, appearing 1,842 and 32,781 and 1 times, respectively. The sequences are further divided into 21 *Orders*, 476 *Families*, 896 *Subfamilies*, 1,355 *Tribes*, 3,855 *Genera* and 10,985 *Species*, 3,025 of which have a single reference sequence associated to them.

Figure 2 depicts the pairwise raw DNA similarities, calculated as the fraction of locations with equal nucleotides, between 3,000 randomly sampled sequences from the library. Each row/column represents the DNA similarity between one sequence and all the other sampled ones, with darker tones indicating higher similarities. Sequences are sorted according to the alphabetical order of their annotation to ensure a cluster separation. In particular, boxes in dark blue along the main diagonal highlight the cross similarities within the *Orders*, while boxes in light blue refer to the *Families*. On the left side of the Figure we report the name and the sizes of the 5 most frequent orders, namely *Araneae*, *Diptera*, *Coleoptera*, *Hymenoptera* and *Lepidoptera*. In an ideal setting, the within-taxon similarities along the main diagonal should be higher than the cross-taxon ones. However, this is only true for *Lepidoptera* and for the two largest families - *Ichneumonidae* and *Tenthredinidae* - in *Hymenoptera*. Indeed, *Diptera* and *Coleoptera* are virtually indistinguishable, as they show a similar within- and between-order similarity. Moreover, these two taxa show a high cross-similarity with *Lepidoptera*, as indicated by the off-diagonal orange rectangles. Overall, the average DNA similarity in the library is around 0.81, indicating that the sequences are highly homogeneous.

¹<https://en.finbol.org/>

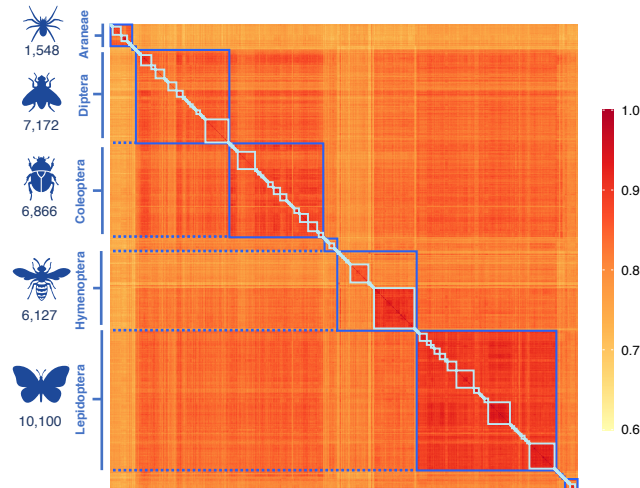


Figure 2: Raw DNA similarities between 3,000 randomly sampled sequences from the FinBOL library. The blue and light blue boxes along the main diagonal identify the *Orders* and the *Families*, respectively. Numbers on the left side represent the frequencies for the 5 largest *Orders* in the data.

3.2 TESTING SCENARIOS

Our aim is to evaluate the performance of the predictive taxa classification probabilities produced by BayesANT. If a sequence is from an existing taxon at a certain rank, that taxon should be assigned relatively high probability. If the sequence is instead from a new taxa, the predictive probabilities should reflect this reality. We train the classifiers on a random subset of 80% of the FinBOL data and predict the taxonomic affiliation for the remaining 20% of the sequences. Some taxa in the test set will not appear in the training data; most existing methods will automatically misclassify these sequences as belonging to one of the taxa in the training library.

We consider two testing scenarios summarized in Figure 3. In the first, each sequence in the library has equal probability of being allocated to the test set. This makes the taxonomic composition of the training and test set similar. As a result, only a relatively small fraction of the taxa will be unobserved in training, as is evident from the top panel of Figure 3. In the second scenario, we create the test set by stratified sampling: for each test observation, we first sample the *Family*, and then draw one sequence within that *Family*. This assigns each *Family* an equal probability of being selected, irrespective of its frequency of appearance in the data. Such a procedure yields a different composition between training and test, resulting in many more test taxa that are unobserved in training. See Figure 3, bottom panel.

3.3 RESULTS

BayesANT computes the probability of every node in the taxonomic tree, including potential novel ones, for every test DNA sequence. The predicted annotation is the taxonomic branch with the highest probability at every rank. These probabilities express the uncertainty of the classification, and need to be well calibrated to be reliable: for instance, if 90% of the sequences are correctly classified, then

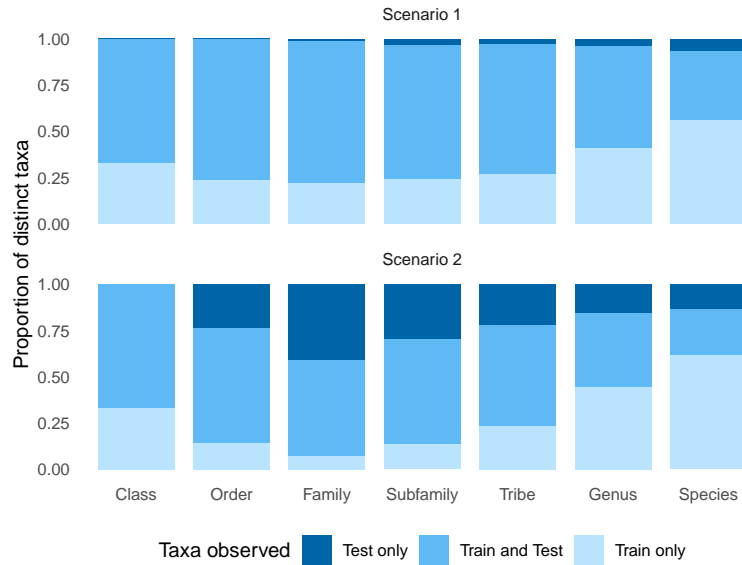


Figure 3: Taxonomic composition of the training and the test libraries in the two splitting scenarios.

the average probability with which they are classified should be around 0.9. Ideally, we would like to limit cases in which the algorithm is too confident when wrong and too conservative when right; see the Materials and Methods section. Moreover, evaluating the performance of BayesANT requires a clear definition of correctness of the classification under novel taxa. If the true annotation of a test sequence shows a taxon which is unobserved in training, the prediction outcome may be the correct novel taxonomic leaf, or a new taxon but in an incorrect branch, or a taxon observed in training. We consider the classification to be correct in the first case and wrong otherwise. For example, if the true annotation of test sequence is

Insecta -> Diptera-> Tephritidae -> Trypetinae -> Trypetini -> Acidia -> Acidia cognata

but *Acidia* is a *Genus* not observed in the training set, then the correct classification up to the *Species* rank is

Insecta -> Diptera -> Tephritidae -> Trypetinae -> Trypetini -> New Genus in Trypetini
-> New Species in New Genus in Trypetini

since the novelty produces a new *Genus* and automatically a new *Species* linked to it. As *Acidia* is not observed, necessarily also the *Species* *Acidia cognata* is unseen and the classification at the *Species* level is correct only if BayesANT recognizes the novel *Genus*. An outcome such as

Insecta -> Diptera -> Tephritidae -> Trypetinae -> Trypetini -> Trypeta
-> New Species in Trypeta

is wrong but recognizes a novel leaf, while

Insecta -> Diptera -> Tephritidae -> Trypetinae -> Trypetini -> Trypeta -> Trypeta zoe

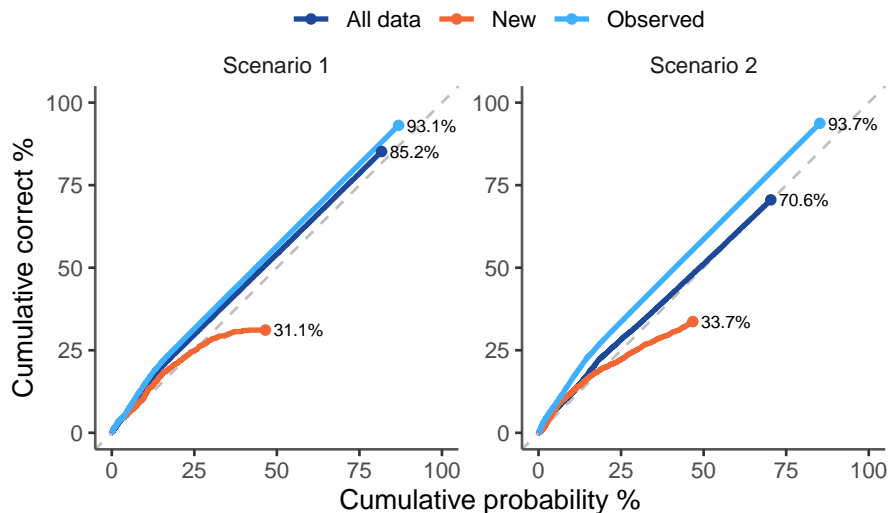


Figure 4: Calibration plot for the prediction of BayesANT at the *Species* level under both scenarios. The dashed diagonal line indicates perfect calibration, while the percentages next to the points are the *Species* accuracies in the test sets. Notice that “All data” includes all the query sequences in the test set, “New” refers to those whose true taxon is not observed in training at some rank, while “Observed” restricts to the cases where the true taxonomy is fully observed.

is wrong since it predicts an observed *Species*.

Figure 4 displays the prediction probabilities of BayesANT in both FinBOL scenarios. As the library is globally aligned, we adopt a simple product-multinomial kernel in which the probabilities of nucleotides “A”, “C”, “G” and “T” vary by loci and species. We treat the alignment gap “-” as a missing value and ignore the likelihood contribution of the locations where it appears. The rank-specific parameters α_ℓ and σ_ℓ are estimated from the data as we detail in the Supplementary material. Figure 4 depicts the relationship between the % cumulative probability and the % cumulative accuracy at the *Species* level. The dashed diagonal indicates a perfectly calibrated output, while trajectories below and above it imply over- and under-confidence, respectively. The dark blue lines show that BayesANT produces well calibrated predictive probabilities on the test data, with a prediction accuracy equal to 85.2% and 70.6% and an average prediction probability of 0.82 and 0.70 in Scenarios 1 and 2, respectively. Results are based on adjusting initial probabilities with a temperature parameter ρ , trained on a hold-out dataset; see Materials and Methods. For the novel cases, the number of sequences predicted to belong to a “new” leaf in Scenario 1 is 958, while their true number is 884. Of these, 77.9% are correctly recognized as novel, and 31.1% are effectively correct up to the *Species* level, with average probability equal to 0.44 as depicted by the orange line. This implies that, while the exact “new” leaf in the taxonomy is generally difficult to retrieve, BayesANT recognizes fairly well the potential novelty of the taxon of a sequence. Verification of the correctness of the novel branch requires further investigation - for example, by morphological assessment and/or more comprehensive sequencing of new samples collected at the same geographic location. Similar results are obtained in Scenario 2.

While accuracy is lower due to a higher number of sequences with unobserved taxa, the predicted novel leaves are 2,736 against 2,672 truly “new”. Here, 93.8% are recognized novel, and 33.7% are fully correct.

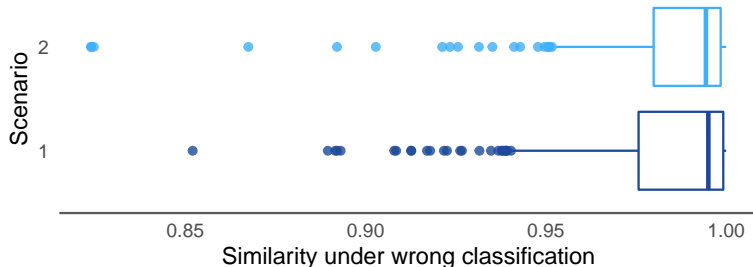


Figure 5: Average DNA similarity between the test query sequences and the predicted taxa when BayesANT incorrectly predicts a taxon observed in training.

In considering these taxonomic classification results, it is important to keep in mind the limited information provided by the available nucleotide sequencing in the COI gene. This information can be insufficient to accurately assign certain query sequences to the correct taxon. To investigate whether this lack of information is a primary cause when BayesANT produces incorrect classifications, we measured the average similarity between the query test sequence and the sequences in the training which are annotated with the predicted taxa when the classification is wrong. Figure 5 shows the distribution of these average similarities. Indeed, these are generally high, with an average of 0.983 under both Scenarios. This implies that misclassification tends to be due to insufficient information to distinguish between the true taxon and an incorrect taxon that is extremely close in the COI region to the query sequence. The ability of BayesANT to provide accurate predictive probabilities is a major advantage in this limited information setting.

3.4 PREDICTION ACCURACIES

As a last step in our analysis, we benchmark the performance of BayesANT on the FinBOL library against several alternatives in terms of accuracy. Table 1 reports the results under both Scenarios. M-1 refers to the single location multinomial kernel we adopted in our analysis above. While this is our method of reference due to its simplicity and flexibility, it treats loci as independent. Dependence can be introduced by adopting a 2-mer location kernel, M-2, where the support of the multinomial is in $\{AA, AC, AT, \dots, TT\}$ and 2-mers are overlapping. See the Materials and Methods section for details. To assess the advantage of adopting a Pitman–Yor prior over the taxonomic tree, we also compare with an analysis that lets $\alpha_\ell = \sigma_\ell = 0$ at every level ℓ . This does not allow new species, and the prior is the proportion with which each taxon appears in the library at every rank. These methods are labelled

MODEL	SCENARIO 1 - PURE RANDOM SPLIT							SCENARIO 2 - STRATIFIED RANDOM SPLIT						
	CLASS	ORDER	FAMILY	SUBFAMILY	TRIBE	GENUS	SPECIES	CLASS	ORDER	FAMILY	SUBFAMILY	TRIBE	GENUS	SPECIES
M-1	<u>100.0</u>	<u>99.9</u>	<u>98.6</u>	<u>97.5</u>	96.0	92.1	85.2	<u>99.8</u>	97.0	<u>82.6</u>	<u>80.8</u>	<u>79.7</u>	75.3	<u>70.6</u>
	(1)	(1)	(.98)	(.96)	(.94)	(.91)	(.82)	(.99)	(.97)	(.87)	(.83)	(.8)	(.77)	(.7)
M-2	<u>100.0</u>	<u>99.9</u>	98.4	97.2	95.8	92.4	<u>85.4</u>	<u>99.8</u>	<u>97.1</u>	82.1	80.3	79.1	<u>75.7</u>	69.8
	(1)	(1)	(.98)	(.97)	(.95)	(.93)	(.86)	(.98)	(.96)	(.88)	(.84)	(.81)	(.8)	(.74)
M-1, NO NEW	<u>100.0</u>	99.5	98.0	97.2	<u>96.7</u>	<u>94.3</u>	83.3	98.7	91.8	75.8	75.3	74.6	72.1	59.4
	(1)	(1)	(.99)	(.98)	(.98)	(.98)	(.92)	(1)	(.98)	(.91)	(.89)	(.89)	(.88)	(.78)
M-2, NO NEW	<u>100.0</u>	99.5	97.5	96.7	96.2	93.8	83.2	96.8	89.3	73.8	73.3	72.8	70.8	59.1
	(1)	(1)	(.99)	(.98)	(.98)	(.98)	(.91)	(1)	(.98)	(.91)	(.89)	(.89)	(.88)	(.74)
RDP	<u>100.0</u>	99.6	97.9	97.1	<u>96.7</u>	94.2	83.1	99.6	95.1	77.8	76.9	76.1	72.9	58.9
	(1)	(.99)	(.97)	(.96)	(.95)	(.94)	(.92)	(.99)	(.92)	(.79)	(.78)	(.77)	(.75)	(.73)

Table 1: Overall predictive performances of DNA barcoding algorithms on the FinBOL library under the two testing scenarios. Values report the % of DNA sequences correctly labelled, while values in parenthesis denote the average prediction probabilities in the whole test set. Underlined values indicate the best performances.

as M-1, NO NEW and M-2, NO NEW in the Table. Finally, we benchmark all these alternatives against the popular RDP classifier (Wang et al., 2007, version 2.13, 2020).

We first notice that no method is uniformly better than the others. Indeed, performances in Scenario 1 are approximately similar both in terms of prediction probabilities and accuracy. Minor differences are found at the *Species* level, where the inclusion of novel taxa leads to higher accuracy for both M-1 and M-2. Under novel taxa, all other methods are necessarily wrong. Moreover, the algorithms show a similar behavior in Scenario 2, which features a much higher proportion of unobserved taxa in training, with the exception of the *Species* level. Here, BayesANT shows its advantage, as it attains a prediction that is 10% more accurate than the RDP classifier. When we restrict to the *Species* observed in training, however, model M-1 shows an accuracy of 93.1% in Scenario 1 and of 93.7% in Scenario 2, while RDP shows 95.3% and 95.9%, respectively. The better performance of RDP under observed *Species* is a consequence of the inclusion of taxonomic novelty, since extending the set of predictable taxa lowers their prior probability. Thus, BayesANT pays a price in terms of accuracy under observed taxa in favor of a much higher gain overall. Indeed, if we neglect novelty in BayesANT, the accuracies of M-1, NO NEW on the observed *Species* are 95.5% and 96.7%.

4 DISCUSSION

This article has proposed a new probabilistic taxonomic classifier, BayesANT, which has the key property of allowing one to probabilistically build on an existing taxonomic library. This is motivated by the fact that existing libraries for arthropods are incomplete, containing reference DNA sequences for a subset of the nodes of the taxonomic tree. Some nodes lacking reference sequences correspond to branches of the tree not yet known to science. For example, it is estimated that approximately 1.5 million, 5.5 million, and 7 million species of beetles, insects, and terrestrial arthropods, respectively, are either awaiting a proper description or are simply undiscovered (Stork, 2018), with estimates varying every year. BayesANT uses species sampling priors (Pitman, 1996) to allow for discovery of previously

unknown branches of the tree, while characterizing uncertainty in all aspects of taxonomic classification including discovery of new species.

Given that taxonomic classification in ecology studies typically relies on sequencing of a relatively short region of the genome, there is necessarily substantial uncertainty in classification (Pentinsaari et al., 2020). For example, different species often have indistinguishable nucleotide sequences in the region being sequenced, so that it becomes impossible to reliably distinguish sequences from such species relying on DNA metabarcoding alone without supplemental morphology data. Hence, it is crucial that taxonomic classifiers provide a realistic measure of uncertainty in classification (Somervuo et al., 2016). Probabilistic forecasts providing accurate characterizations of predictive uncertainty are said to be well calibrated. BayesANT guarantees well calibrated predictions through a cross validation approach.

BayesANT builds on a popular species sampling prior known as the Pitman-Yor process (Perman et al., 1992). The classical Pitman-Yor process does not take into account the taxonomic tree structure, and instead treats all species as exchangeable. However, by using a Pitman-Yor at each level of the tree, with different parameters for each taxonomic rank, we obtain a highly flexible generative probabilistic process that can predict the probability of a new query sequence belonging to a different taxa at each level of the tree. By estimating the Pitman-Yor parameters based on the training data, we allow the process to adapt to existing knowledge about the level of diversity at each taxonomic rank.

The modeling choices made in building BayesANT reflect a balance between flexibility and pragmatism in developing an efficient off-the-shelf algorithm that can easily handle classification of millions of sequences. This is needed in our motivating applications to biodiversity monitoring studies that routinely collect and metabarcode samples from many different sites and multiple time points for each site. In future research, it may be helpful to consider other modeling choices, which modify the Pitman-Yor structure and/or choices of kernels considered here. For example, instead of the simple multinomial kernels, it may be useful to explore similarity and latent variable-based likelihoods, for example using the projected κ -mer decomposition of a sequence into a lower dimensional feature space.

Taxonomic novelty due to missing branches in the reference libraries is discussed in the literature (Lan et al., 2012; Somervuo et al., 2017). Interpretation of the detected “new”, however, is fairly delicate and context dependent, and requires further investigation on the sequenced DNA. It is common in practice to ignore the query sequences that show classification confidence below a certain threshold. Such an approach can be effective in removing reads suspected of sequencing error. However, it is unclear whether a low classification probability to existing taxa implies the sequence is likely from a novel taxa. BayesANT provides a probabilistic framework for avoiding such arbitrary thresholds, instead characterizing uncertainty in all aspects of classification including to new branches of the tree.

two taxa at the *Order* level: one that has a butterfly-type morphological trait, $V_{1,1}^*$, and one with a bee-type trait, $V_{2,1}^*$. The beetle-shaped insect node instead represents a potential *Order* yet to be discovered.

Due to the tree structure of the taxonomy, each generic node v_ℓ at level ℓ has a unique parent at level $\ell - 1$, denoted as $\text{pa}(v_\ell)$. In Figure 6, for instance, $\text{pa}(V_{1,2}^*) = V_{1,1}^*$ and $\text{pa}(V_{1,3}^*) = \text{pa}(V_{2,3}^*) = V_{1,2}^*$. For coherence, assume that the tree is rooted, namely $\text{pa}(v_1) = v_0$ for any $v_1 \in \mathcal{V}_1$. Each node in the tree is linked to multiple taxa at lower ranks. Let $\rho_n(v_\ell)$ be the set of observed nodes $v_{\ell+1}$ for which $\text{pa}(v_{\ell+1}) = v_\ell$ when n sequences are observed, $K_n(v_\ell) = |\rho_n(v_\ell)|$ be its cardinality and $N_n(v_\ell)$ be the number of DNA sequences belonging to v_ℓ . In Figure 6, $\rho_n(V_{1,2}^*) = \{V_{1,3}^*, V_{2,3}^*\}$ and $K_n(V_{1,2}^*) = 2$, while $\rho_n(v_0) = \{V_{1,1}^*, V_{2,1}^*\}$ and $K_n(v_0) = 2$ for the *Order* level. Finally, the size of a node in our representation is determined as a sum of the number of sequences stored in all leaves connected to it. For example, $N_n(V_{1,2}^*) = 8$, and $N_n(V_{1,1}^*) = 12$. The quantities $\text{pa}(\cdot)$, $\rho_n(\cdot)$, $K_n(\cdot)$ and $N_n(\cdot)$ are the key ingredients upon which we build our taxonomic prior π_v in equation (3).

5.2 TAXONOMIC PRIOR

The first step in our analysis consists of specifying a flexible prior for the frequencies of occurrence of different types of organisms at each taxonomic rank ℓ , including organisms of “new” types. In particular, we incorporate the Pitman–Yor process allocation probabilities in equations (1) and (2) into the tree structure. Let α_ℓ and σ_ℓ denote the allocation parameters for level ℓ , with $\alpha_\ell > -\sigma_\ell$ and $\sigma_\ell \in [0, 1)$. Write $\mathbf{V}_{\cdot,\ell}^{(n)} = (V_{i,\ell})_{i=1}^n$ as the sequence of taxonomic labels observed at level ℓ . Then, the taxon of sequence $n + 1$ at level ℓ , conditioned on it being allocated to node $v_{\ell-1}$ at level $\ell - 1$, has probabilities

$$\text{pr}(V_{n+1,\ell} = V_{j,\ell}^* \mid V_{n+1,\ell-1} = v_{\ell-1}, \mathbf{V}_{\cdot,\ell}^{(n)}) = \frac{N_n(V_{j,\ell}^*) - \sigma_\ell}{\alpha_\ell + N_n(v_{\ell-1})}, \quad (4)$$

if the node $V_{j,\ell}^*$ is such that $\text{pa}(V_{j,\ell}^*) = v_{\ell-1}$, and

$$\text{pr}(V_{n+1,\ell} = \text{“new”} \mid V_{n+1,\ell-1} = v_{\ell-1}, \mathbf{V}_{\cdot,\ell}^{(n)}) = \frac{\alpha_\ell + \sigma_\ell K_n(v_{\ell-1})}{\alpha_\ell + N_n(v_{\ell-1})}, \quad (5)$$

if the node is new and originates from $v_{\ell-1}$. The structure of equations (4) and (5) is the same as the one in equations (1) and (2), with the only difference being that nodes at ℓ are generated from their parent-specific process. The level-specific parameters α_ℓ and σ_ℓ are important in allowing diversity to vary with taxonomic rank. These parameters will be estimated based on the data as we detail in the Supplementary material.

SEQUENCES	METHOD	KERNEL	PRIOR $\boldsymbol{\theta}_{v_L}$
Not aligned	κ -mers	$\prod_{g \in \mathcal{N}_\kappa} \theta_{v_L, g}^{n_{i, g}}$	DIR($\boldsymbol{\xi}_{v_L}$)
Aligned	Product	$\prod_{s=1}^p \prod_{g \in \mathcal{N}_1} \theta_{v_L, s, g}^{\mathbf{1}\{X_{i, s} = g\}}$	$\prod_s \text{DIR}(\boldsymbol{\xi}_{v_L, s})$
Aligned	κ -Product	$\prod_{s=1}^p \prod_{g \in \mathcal{N}_\kappa} \theta_{v_L, s, g}^{\mathbf{1}\{X_{i, s} = g\}}$	$\prod_s \text{DIR}(\boldsymbol{\xi}_{v_L, s})$

Table 2: Examples of multinomial kernels for the DNA sequences. \mathcal{N}_κ is the set of all κ -mers on which the sequence is decomposed. In the aligned case, this is a set of monomers $\mathcal{N}_1 = \{A, C, G, T\}$. The quantity $\mathbf{1}\{X_{i, s} = g\}$ is an indicator equal to one if $X_{i, s} = g$ and zero otherwise.

5.3 DNA SEQUENCE LIKELIHOOD

The second step to build the predictive rule in equation (3) is to specify a distribution for the DNA sequences. We do this by adopting a kernel-based approach that flexibly accommodates different DNA representations.

As depicted in Figure 6, a query sequence \mathbf{X}_i is uniquely associated with one leaf of the taxonomic tree. Recalling that $V_{i, L}$ is the taxon of the i th sequence at the lowest level L , we let

$$(\mathbf{X}_i \mid V_{i, L} = v_L, \boldsymbol{\theta}_{v_L}) \stackrel{\text{iid}}{\sim} \mathcal{K}(\mathbf{X}_i; \boldsymbol{\theta}_{v_L}), \quad (6)$$

where $v_L \in \mathcal{V}_L$ is a generic leaf, $\mathcal{K}(\mathbf{X}_i; \boldsymbol{\theta})$ is a kernel depending on parameters $\boldsymbol{\theta}$ representing the likelihood of sequence data \mathbf{X}_i , and $\boldsymbol{\theta}_{v_L}$ is a collection of leaf-specific parameters. We assume that all DNA sequences associated to leaf v_L are independent and identically distributed as $\mathcal{K}(\cdot; \boldsymbol{\theta}_{v_L})$. Table 2 provides three examples of multinomial-type kernels when sequences are aligned and when they are not. Here, *alignment* implies that all the sequences are pre-processed to have the same length p so that the nucleotides at each position $s = 1, \dots, p$ are meaningfully comparable. Then, $X_{i, s}$ is the nucleotide in the s th position of the i th query sequence, and $\theta_{v_L, s, g}$ is the probability that nucleotide $g \in \mathcal{N}_1 = \{A, C, G, T\}$ is seen at s for taxon v_L . Assuming independence across locations s as a simplifying assumption to improve computational efficiency in constructing a probabilistic classifier, the resulting kernel is a product of multinomials with location-specific parameters.

When sequences are *not* aligned, each has its own length p_i . A viable option is to use a κ -mer decomposition. This amounts to counting the number of times all possible 4^κ substrings of length κ appear within the sequence. We denote as \mathcal{N}_κ the set of all κ -mers of length κ . For instance, 3-mers live in $\mathcal{N}_3 = \{AAA, ACG, AGT \dots\}$, with a total of $4^3 = 64$ substrings. In Table 2, $n_{i, g} = \sum_{s=1}^{t_i} \mathbf{1}\{X_{i, s} = g\}$ denotes the number of times a κ -mer $g \in \mathcal{N}_\kappa$ appears in the i th sequence, with $t_i = p_i - \kappa + 1$ being the total number of κ -mers observed when the length is p_i . We model these counts as the output of a multinomial distribution, where $\theta_{v_L, g}$ is the probability of κ -mer g at taxon v_L .

The choice of kernel depends on the application and on the data. Insect DNA sequences can be easily aligned via hidden Markov models (Eddy, 1995). This is not true for fungal sequences, which are

substantially more diverse and hence difficult if not impossible to align. Irrespective of the structure of the data, our proposed multinomial kernels have the advantage of simplicity in computation, with the posterior distribution for θ_{v_L} obtained in analytic form by adopting conjugate Dirichlet priors as in Table 2. Computational efficiency is a critical issue in classifying very large numbers of sequences, making it intractable to consider elaborate likelihoods derived from realistic generative models of nucleotide sequences.

5.4 PREDICTION RULE

The prior on the tree and the DNA sequence likelihood defined so far allow us to predict the set of labels \mathbf{V}_{n+1} for the query sequence \mathbf{X}_{n+1} . BayesANT does this in *bottom-up* and *top-down* steps. In the *bottom-up* step, we use equations (4), (5) and (6) to determine the posterior probability that \mathbf{X}_{n+1} belongs to *any* leaf in the tree. These include both the observed and the new taxa at the lowest level, as illustrated in Figure 6². Then, probabilities of higher nodes are computed aggregating upward. In the *top-down* step, instead, BayesANT predicts a branch by iteratively choosing the child node with the highest probability at each level, starting from the root.

Let $\pi_{n+1}(v_L)$ be the prior probability of leaf v_L after having observed \mathcal{D}_n . This is equal to the product of the prior conditional probabilities in equations (4) and (5) of all nodes in the branch v_0-v_L , which is

$$\pi_{n+1}(v_L) = \text{pr}(V_{n+1,1} = v_1 \mid \mathbf{V}_{:,1}^{(n)}) \prod_{\ell=2}^L \text{pr}(V_{n+1,\ell} = v_\ell \mid V_{n+1,\ell-1} = v_{\ell-1}, \mathbf{V}_{:, \ell}^{(n)}). \quad (7)$$

Equation (7) is the equivalent of the prior taxon probability in equation (3). Notice that if $v_\ell = \text{“new”}$ at some ℓ , the conditional probabilities at lower nodes are equal to 1. But then, the probability that $V_{n+1,L}$ is associated to taxon v_L *conditioned on the DNA sequence* \mathbf{X}_{n+1} is

$$p_{n+1}(v_L) = \text{pr}(V_{n+1,L} = v_L \mid \mathbf{X}_{n+1}, \mathcal{D}_n) \propto \pi_{n+1}(v_L) \int \mathcal{K}(\mathbf{X}_{n+1}; \boldsymbol{\theta}_{v_L}) p(\boldsymbol{\theta}_{v_L} \mid \mathcal{D}_n) d\boldsymbol{\theta}_{v_L}. \quad (8)$$

The integral in equation (8) is the posterior predictive distribution of DNA sequence \mathbf{X}_{n+1} with respect to the posterior of $\boldsymbol{\theta}_{v_L}$. When $v_\ell = \text{“new”}$, this posterior is equal to the prior, i.e. $p(\boldsymbol{\theta}_{v_L} \mid \mathcal{D}_n) = p(\boldsymbol{\theta}_{v_L})$, as no sequence for v_L is observed. The advantage of the models in Table 2 is that both the prior and the posterior predictive distribution have simple and easy-to-compute analytic forms.

Once equation (8) has been evaluated for all leaves, the probabilities of higher nodes in the taxonomy can be easily derived via upward aggregation. Then, we predict the taxa by starting from the root of the tree and recursively selecting the child node with the highest probability. Specifically, the predicted

²Under the assumption that a new node at level ℓ automatically creates a new node at all levels $\ell + 1, \dots, L$ below, the total number of potentially unobserved leaves is equal to the number of nodes up to $L - 1$ plus 1

sequence of taxa $(v_\ell^*)_{\ell=1}^L$ for the DNA sequence at $n + 1$ satisfies

$$v_\ell^* = \arg \max_{v_\ell \in \rho_n(v_{\ell-1}^*)} \sum_{v_L \in \mathcal{L}_n(v_\ell)} p_{n+1}(v_L), \quad (9)$$

where $\mathcal{L}_n(v_\ell)$ is the set of all leaves linked to node v_ℓ in a library of n DNA sequences.

5.5 HYPERPARAMETER TUNING

The hyperparameters ξ_v of the multinomial kernel play a fundamental role in novel species recognition. As detailed above, when $v_L = \text{“new”}$, then equation (8) is a prior predictive probability, since no sequence is observed for v_L and thus $p(\theta_{v_L} | \mathcal{D}_n) = p(\theta_{v_L})$. In such cases, prior hyperparameters should contain information regarding the taxonomic branch and level where novelty appears. Uniform priors may be unreasonably vague, leading to under-estimation of the prior predictive probability of novel taxa relative to the true proportion. Thus, we tune each ξ_{v_L} as follows. Consider a taxon v_{L-1} at level $L - 1$. If v_{L-1} is not “new”, the hyperparameters ξ_{v_L} of all the leaves $v_L \in \mathcal{L}_n(v_{L-1})$ linked to it - including the new one - are all equal, and they are obtained via method of the moments from the DNA sequences \mathbf{X}_i with $V_{i,L-1} = v_{L-1}$. If instead v_{L-1} is a “new” node and the last not novel node in its branch is v_ℓ at level $\ell \leq L - 1$, the method of the moments is applied on the set of sequences \mathbf{X}_i such that $V_{i,\ell} = v_\ell$. This ensures borrowing of information between the branches when the novelty appears at higher levels in the taxonomy. For mathematical details on the method of the moments applied to the multinomial kernels of Table 2, see the Supplementary material.

5.6 CALIBRATION OF PREDICTION PROBABILITIES

Misspecification of a Bayesian model, due to inaccuracies in the prior and/or likelihood function, may lead to predictive probabilities that are not sufficiently well calibrated to accurately capture predictive uncertainties (Grünwald and van Ommen, 2017; Miller and Dunson, 2019). Given the complexity of the true data-generating likelihood underlying DNA barcoding data, and the necessity of using a simple likelihood for computational tractability, some degree of misspecification is inevitable. To adjust the predictive probabilities used in equation (9) for misspecification, we apply a simple re-calibration approach. In particular, we post-process the prediction probabilities in equation (8) by exponentiating them by a coefficient $\rho \in (0, 1]$ and later renormalizing. Then, the new probabilities for the $(n + 1)$ st sequence are

$$\tilde{p}_{n+1}(v_L) = \frac{p_{n+1}(v_L)^\rho}{\sum_{v \in \mathcal{V}_L} p_{n+1}(v)^\rho}, \quad (10)$$

and can be used in place of $p_{n+1}(v_L)$ in equation (9). Such a strategy does not alter the ranking of the original probabilities since the transformation is monotonic. Moreover, if $p_{n+1}(v_L) = 1$, then also

$\tilde{p}_{n+1}(v_L) = 1$. This implies that we do not substantially alter the prediction whenever the BayesANT is certain about a taxon. Choices for ρ can be adopted via cross validation on an hold-out subset of the training library following strategies such as the ones described in (Guo et al., 2017). Specifically, prediction probabilities are calibrated if the average probability for the predicted nodes is equal to the classification accuracy (Somervuo et al., 2016). For example, if 90% of the sequences are correctly classified, ideally the average classification probability is approximately 0.9. An average value of 0.5 and of 0.99, instead, means that the algorithm is too conservative when right and too confident when wrong, respectively. We select $\rho = 0.1$ under both Scenarios of the FinBOL application. In general, our experience suggests that $\rho \approx 0.1$ works well in practice with other libraries as well.

SOFTWARE AVAILABILITY

BayesANT is available as an open-source R package at <https://alessandrozito.github.io/BayesANT/vignette.html>.

DATA AVAILABILITY

We use the full COI version of the library available at <https://github.com/psomervuo/FinPROTAX>. We restrict to sequences with fully specified taxonomy up to the *Species* level.

ACKNOWLEDGEMENTS

This project has received funding from the European Research Council under the European Union’s Horizon 2020 research and innovation programme (grant agreement No 856506). The authors would like to express their gratitude to Otso Ovaskainen, Panu Somervuo, Jesse Harrison, Markus Koskela, Tomas Roslin, Bianca Dumitrascu and Jennifer Kampe for their precious suggestions, to Elena Domenichini for graphical advice and to Carolyn Quarterman for the support on the writing.

REFERENCES

- Altschul, S. F., W. Gish, W. Miller, E. W. Myers, and D. J. Lipman (1990). Basic local alignment search tool. *Journal of Molecular Biology* 215(3), 403–410.
- Bazinet, A. L. and M. P. Cummings (2012). A comparative evaluation of sequence classification programs. *BMC Bioinformatics* 13(1), 92.
- Blackwell, D. and J. B. MacQueen (1973). Ferguson distributions via Pólya urn schemes. *Annals of Statistics* 1(2), 353–355.

- De Blasi, P., S. Favaro, A. Lijoi, R. H. Mena, I. Prünster, and M. Ruggiero (2015). Are Gibbs-type priors the most natural generalization of the Dirichlet process? *IEEE Transactions on Pattern Analysis and Machine Intelligence* 37(2), 212–229.
- Eddy, S. R. (1995). Multiple alignment using hidden markov models. *Proceedings. International Conference on Intelligent Systems for Molecular Biology 3*, 114–120.
- Edgar, R. C. (2013). Uparse: highly accurate otu sequences from microbial amplicon reads. *Nature Methods* 10(10), 996–998.
- Favaro, S., A. Lijoi, R. H. Mena, and I. Prünster (2009). Bayesian non-parametric inference for species variety with a two-parameter Poisson–Dirichlet process prior. *Journal of the Royal Statistical Society, Series B* 71(5), 993–1008.
- FinBIF (2020). *The FinBIF checklist of Finnish species 2019*. Finnish Biodiversity Information Facility, Finnish Museum of Natural History, University of Helsinki. Retrieved from <http://urn.fi/URN:ISSN:2490-0907>.
- Grünwald, P. and T. van Ommen (2017). Inconsistency of Bayesian Inference for Misspecified Linear Models, and a Proposal for Repairing It. *Bayesian Analysis* 12(4), 1069–1103.
- Guo, C., G. Pleiss, Y. Sun, and K. Q. Weinberger (2017). On calibration of modern neural networks. In *Proceedings of the 34th International Conference on Machine Learning - Volume 70, ICML’17*, pp. 1321–1330.
- Hebert, P. D. N., A. Cywinska, S. Ball, and J. deWaard (2003). Biological identifications through DNA barcodes. *Journal of the Royal Statistical society of London B: Biological Sciences* 270, 313–321.
- Huson, D. H., A. F. Auch, J. Qi, and S. C. Schuster (2007). Megan analysis of metagenomic data. *Genome research* 17(3), 377–386.
- Janzen, D. H., M. Hajibabaei, J. M. Burns, W. Hallwachs, E. Remigio, and P. D. N. Hebert (2005). Wedding biodiversity inventory of a large and complex Lepidoptera fauna with DNA barcoding. *Philosophical Transactions of the Royal Society B* 360, 1835–1845.
- Lan, Y., Q. Wang, J. R. Cole, and G. L. Rosen (2012). Using the RDP classifier to predict taxonomic novelty and reduce the search space for finding novel organisms. *PLOS ONE* 7(3), 1–15.
- Lijoi, A., R. H. Mena, and I. Prünster (2007). Bayesian nonparametric estimation of the probability of discovering new species. *Biometrika* 94(4), 769–786.
- Malaise, R. (1937). A new insect-trap. *Entomologisk Tidskrift* 58, 148–160.

- Miller, J. W. and D. B. Dunson (2019). Robust bayesian inference via coarsening. *Journal of the American Statistical Association* 114(527), 1113–1125.
- Nguyen, N.-P., S. Mirarab, B. Liu, M. Pop, and T. Warnow (2014). TIPP: taxonomic identification and phylogenetic profiling. *Bioinformatics* 30(24), 3548–3555.
- Pentinsaari, M., S. Ratnasingham, S. E. Miller, and P. D. N. Hebert (2020). Bold and genbank revisited – do identification errors arise in the lab or in the sequence libraries? *PLoS One* 15(4), 1–10.
- Perman, M., J. Pitman, and M. Yor (1992). Size-biased sampling of Poisson point processes and excursions. *Probability Theory and Related Fields* 92(1), 21–39.
- Pitman, J. (1996). Some developments of the Blackwell-MacQueen urn scheme. In T. S. Ferguson, L. S. Shapley, and J. B. MacQueen (Eds.), *Statistics, Probability and Game Theory. Papers in honor of David Blackwell*, Volume 30 of *IMS Lecture notes, Monograph Series*, pp. 245–267. Hayward: Institute of Mathematical Statistics.
- Ratnasingham, S. and P. D. N. Hebert (2013). A DNA-based registry for all animal species: the Barcode Index Number (BIN) system. *PLoS ONE* 8(7), e66213.
- Roslin, T., P. Somervuo, M. Pentinsaari, P. D. N. Hebert, J. Agda, P. Ahlroth, P. Anttonen, J. Aspi, G. Blagoev, S. Blanco, D. Chan, T. Clayhills, J. deWaard, S. deWaard, T. Elliot, R. Elo, S. Haapala, E. Helve, J. Imonen, ..., and M. Mutanen (2022). A molecular-based identification resource for the arthropods of Finland. *Molecular Ecology Resources* 22(2), 803–822.
- Sarkar, I. and M. Trizna (2011). The Barcode of Life data portal: bridging the biodiversity informatics divide for DNA barcoding. *PLoS ONE* 6, e14689.
- Seibold, S., M. M. Gossner, N. K. Simons, N. Blüthgen, J. Müller, D. Ambarli, C. Ammer, J. Bauhus, M. Fischer, J. C. Habel, K. E. Linsenmair, T. Naus, C. Penone, D. Prati, P. Schall, E.-D. Schulze, J. Vogt, S. Wöllauer, and W. W. Weisser (2019). Arthropod decline in grasslands and forests is associated with landscape-level drivers. *Annual Review of Entomology* 574, 671–674.
- Shokralla, S., J. Gibson, H. Nikbakht, D. Janzen, W. Hallwachs, and M. Hajibabaei (2014). Next-generation dna barcoding: using next-generation sequencing to enhance and accelerate dna barcode capture from single specimens. *Molecular Ecology Resources* 5, 892–901.
- Somervuo, P., S. Koskela, J. Pennanen, R. Henrik Nilsson, and O. Ovaskainen (2016). Unbiased probabilistic taxonomic classification for DNA barcoding. *Bioinformatics* 32(19), 2920–2927.

- Somervuo, P., D. W. Yu, C. C. Xu, Y. Ji, J. Hultman, H. Wirta, and O. Ovaskainen (2017). Quantifying uncertainty of taxonomic placement in dna barcoding and metabarcoding. *Methods in Ecology and Evolution* 8(4), 398–407.
- Stork, N. E. (2018). How many species of insects and other terrestrial arthropods are there on earth? *Annual Review of Entomology* 63(1), 31–45.
- Vu, D., M. Groenewald, and G. Verkley (2020). Convolutional neural networks improve fungal classification. *Scientific Reports* 10, 12628.
- Wang, Q., G. M. Garrity, J. M. Tiedje, and J. R. Cole (2007). Naive bayesian classifier for rapid assignment of rRNA sequences into the new bacterial taxonomy. *Applied and environmental microbiology* 73(16), 5261–5267.
- Wilson, J.-J., K.-W. Sing, R. M. Floyd, and P. D. N. Hebert (2017). *DNA Barcodes and Insect Biodiversity*, Chapter 17, pp. 575–592. John Wiley & Sons, Ltd.
- Yu, D. W., Y. Ji, B. C. Emerson, X. Wang, C. Ye, C. Yang, and Z. Ding (2012). Biodiversity soup: metabarcoding of arthropods for rapid biodiversity assessment and biomonitoring. *Methods in Ecology and Evolution* 3(4), 613–623.
- Zito, A., T. Rigon, O. Ovaskainen, and D. Dunson (2020). Bayesian nonparametric modelling of sequential discoveries. *arXiv:2011.06629*.

SUPPLEMENTARY MATERIAL

The following document contains mathematical and theoretical details for the BayesANT algorithm - BAYESiAn Nonparametric Taxonomic classifier - described in the main paper. Emphasis is on the explicit formulas for the taxonomic annotation probabilities and the associated estimation method for the model parameters.

A PRIOR TAXONOMIC PROBABILITIES

In this section we provide details on the prior probabilities over the nodes in the taxonomic tree, and describe the estimation procedure for the associated hyperparameters.

A.1 THE PITMAN–YOR PROCESS AND THE EXCHANGEABLE PARTITION PROBABILITY FUNCTION

BayesANT models taxonomic novelty via Pitman–Yor process priors (Perman et al., 1992). As already detailed in the main paper, the process works as follows. Let V_1, \dots, V_n be a sequence of taxon assignments for the DNA sequences in the training library, comprising of a total of $K_n = k$ distinct labels denoted as V_1^*, \dots, V_k^* and appearing with frequencies n_1, \dots, n_k . Then, the taxon of the $(n+1)$ st observation is determined via the following allocation scheme:

$$(V_{n+1} | V_1, \dots, V_n) = \begin{cases} V_j^*, & \text{with prob. } (n_j - \sigma)/(\alpha + n), \quad j = 1, \dots, k, \\ \text{“new”}, & \text{with prob. } (\alpha + \sigma k)/(\alpha + n), \end{cases} \quad (11)$$

where $\sigma \in [0, 1)$ is a discount parameter governing the tail of the process and $\alpha > -\sigma$ is a precision parameter. High values for α and σ lead to a high number of distinct labels K_n . Moreover, high values for n_j lead to a high probability that taxon V_j^* will be observed in the future. See Figure 1 in the main paper for a practical illustration. Estimation of both parameters can be performed via an empirical Bayes procedure (Favaro et al., 2009) through maximization of the quantity known as *exchangeable partition probability function* (EPPF, Pitman, 1996). Let N_j denote the random variable corresponding to the frequency of appearance of taxon V_j^* , with n_j the realization of this random variable for $K_n = k$. The EPPF is defined as

$$\text{pr}(K_n = k, N_1 = n_1, \dots, N_k = n_k) = \frac{\prod_{i=1}^{k-1} (\alpha + i\sigma)}{(\alpha + 1)_{n-1}} \prod_{j=1}^k (1 - \sigma)_{n_j - 1}, \quad (12)$$

where $(x)_a = \Gamma(x+a)/\Gamma(x)$ is the Pochhammer factorial and $\Gamma(x)$ is the gamma function. The quantity in equation (12) can be interpreted as a likelihood function arising from the process in equation (11).

Then, one can simply apply maximum likelihood estimation as

$$(\hat{\alpha}, \hat{\sigma}) = \arg \max_{\alpha, \sigma} \left\{ \frac{\prod_{i=1}^{k-1} (\alpha + i\sigma)}{(\alpha + 1)_{n-1}} \prod_{j=1}^k (1 - \sigma)_{n_{j-1}} \right\}, \quad \sigma \in [0, 1), \alpha > -\sigma.$$

In what follows, we apply this procedure to estimate the parameters α_ℓ and σ_ℓ for all levels $\ell = 1, \dots, L$ in the taxonomic tree.

A.2 LEVEL-SPECIFIC PITMAN–YOR PRIORS

Consider a taxonomic library $\mathcal{D}_n = (\mathbf{V}_i, \mathbf{X}_i)_{i=1}^n$ of size n and of $L \geq 2$ levels, where $\mathbf{V}_i = (V_{i,\ell})_{\ell=1}^L$ are the taxonomic annotations for DNA sequence \mathbf{X}_i . Following the notation in the main paper, we let $V_{j,\ell}^*$ be the j th taxon and $\mathbf{V}_{\cdot,\ell}^{(n)} = (V_{i,\ell})_{i=1}^n$ be the sequence of taxa observed for level ℓ . To construct the taxonomic tree, we introduce the following quantities. For a generic taxon v_ℓ at level ℓ , we define $\text{pa}(v_\ell)$ as the unique parent node of v_ℓ at level $\ell - 1$ and $\rho_n(v_\ell)$ as the set of nodes $v_{\ell+1}$ at level $\ell + 1$ such that $\text{pa}(v_{\ell+1}) = v_\ell$. We also let $K_n(v_\ell) = |\rho_n(v_\ell)|$ be the number of nodes linked to v_ℓ at level $\ell + 1$ and $N_n(v_\ell)$ be the size of the taxon, namely the number of DNA sequences linked to v_ℓ . Then, BayesANT follows the prediction scheme in equation (11) by letting

$$(V_{n+1,\ell} \mid V_{n+1,\ell-1} = v_{\ell-1}, \mathbf{V}_{\cdot,\ell}^{(n)}) = \begin{cases} V_{j,\ell}^*, & \text{with prob. } (N_n(V_{j,\ell}^*) - \sigma_\ell) / (\alpha_\ell + N_n(v_{\ell-1})), \\ \text{“new”}, & \text{with prob. } (\alpha_\ell + \sigma_\ell K_n(v_{\ell-1})) / (\alpha_\ell + N_n(v_{\ell-1})), \end{cases} \quad (13)$$

for $j : \text{pa}(V_{j,\ell}^*) = v_{\ell-1}$, where $\sigma_\ell \in [0, 1)$ and $\alpha_\ell > -\sigma_\ell$ are rank-specific parameters. Equation (13) holds independently for all the observed nodes $v_{\ell-1}$ at level $\ell - 1$. Specifically, we model all the separate sets of taxa $\rho_n(v_{\ell-1})$ at a given rank ℓ as realizations from independent Pitman–Yor processes. In estimating parameters α_ℓ, σ_ℓ , we borrow of information across branches. The level-specific EPPF is a product EPPFs, and the estimates for α_ℓ and σ_ℓ are obtained as

$$(\hat{\alpha}_\ell, \hat{\sigma}_\ell) = \arg \max_{\alpha_\ell, \sigma_\ell} \left\{ \prod_{v \in \mathcal{V}_{\ell-1}} \frac{\prod_{i=1}^{K_n(v)-1} (\alpha_\ell + i\sigma_\ell)}{(\alpha_\ell + 1)_{N_n(v)-1}} \prod_{v_\ell \in \rho_n(v)} (1 - \sigma_\ell)_{N_n(v_\ell)-1} \right\}, \quad (14)$$

for $\sigma_\ell \in [0, 1), \alpha_\ell > -\sigma_\ell$, where $\mathcal{V}_{\ell-1}$ denotes the set of all taxonomic nodes $V_{j,\ell-1}^*$ observed in the library at level $\ell - 1$. The maximization in equation (14) can easily be carried out with routine methods such as `nlmminb` in R.

A.3 LEAF PROBABILITIES

After α_ℓ and σ_ℓ have been estimated from the library \mathcal{D}_n , BayesANT specifies the prior probability for each leaf node $v_L \in \mathcal{V}_L$, including new ones, as a product of Pitman–Yor probabilities. For the

$(n + 1)$ st sequence, this is equal to

$$\begin{aligned}\pi_{n+1}(v_L) &= \text{pr}(V_{n+1,L} = v_L \mid \mathcal{D}_n) \\ &= \text{pr}(V_{n+1,1} = v_1 \mid \mathbf{V}_{:,1}^{(n)}) \times \prod_{\ell=2}^L \text{pr}(V_{n+1,\ell} = v_\ell \mid V_{n+1,\ell-1} = v_{\ell-1}, \mathbf{V}_{:, \ell}^{(n)}).\end{aligned}\tag{15}$$

To see this explicitly, consider the example of a $L = 4$ level library of size n and let $V_{1,1}^* \rightarrow V_{1,2}^* \rightarrow V_{1,3}^* \rightarrow V_{1,4}^*$ be a branch. This is a fully observed branch, for which $\text{pa}(V_{1,2}^*) = V_{1,1}^*$, $\text{pa}(V_{1,3}^*) = V_{1,2}^*$ and $\text{pa}(V_{1,4}^*) = V_{1,3}^*$. Then, the prior probability for the leaf node $V_{1,4}^*$ is

$$\pi_{n+1}(V_{1,4}^*) = \underbrace{\frac{N_n(V_{1,1}^*) - \sigma_1}{\alpha_1 + n}}_{\text{Prob. of choosing } V_{1,1}^* \text{ at Level 1}} \times \underbrace{\frac{N_n(V_{1,2}^*) - \sigma_2}{\alpha_2 + N_n(V_{1,1}^*)}}_{\text{Prob. of choosing } V_{1,2}^* \text{ at Level 2}} \times \underbrace{\frac{N_n(V_{1,3}^*) - \sigma_3}{\alpha_3 + N_n(V_{1,2}^*)}}_{\text{Prob. of choosing } V_{1,3}^* \text{ at Level 3}} \times \underbrace{\frac{N_n(V_{1,4}^*) - \sigma_4}{\alpha_4 + N_n(V_{1,3}^*)}}_{\text{Prob. of choosing } V_{1,4}^* \text{ at Level 4}}.$$

Consider instead the path $V_{1,1}^* \rightarrow V_{1,2}^* \rightarrow \text{“new”} \rightarrow \text{“new”}$. This identifies a new branch at level $\ell = 3$, which in turn creates a new leaf. We denote it as v_L^{new} . Then, its associated probability is

$$\pi_{n+1}(v_L^{\text{new}}) = \underbrace{\frac{N_n(V_{1,1}^*) - \sigma_1}{\alpha_1 + n}}_{\text{Prob. of choosing } V_{1,1}^* \text{ at Level 1}} \times \underbrace{\frac{N_n(V_{1,2}^*) - \sigma_2}{\alpha_2 + N_n(V_{1,1}^*)}}_{\text{Prob. of choosing } V_{1,2}^* \text{ at Level 2}} \times \underbrace{\frac{\alpha_3 + \sigma_3 K_n(V_{1,2}^*)}{\alpha_3 + N_n(V_{1,2}^*)}}_{\text{Prob. of novelty at Level 3}} \times \underbrace{1}_{\text{Prob. of novelty at Level 4}}.$$

Here, the novelty probability of the Pitman–Yor process appears at level 3. At level 4 the probability is equal to one since the node is necessarily new and $K_n(v_L^{\text{new}}) = N_n(v_L^{\text{new}}) = 0$. In a similar fashion, the probability for the branch “new” \rightarrow “new” \rightarrow “new” \rightarrow “new” is

$$\pi_{n+1}(v_L^{\text{new}}) = \underbrace{\frac{\alpha_1 + \sigma_1 K_n(v_0)}{\alpha_1 + n}}_{\text{Prob. of novelty at Level 1}} \times \underbrace{1}_{\text{Prob. of novelty at Level 2}} \times \underbrace{1}_{\text{Prob. of novelty at Level 3}} \times \underbrace{1}_{\text{Prob. of novelty at Level 4}},$$

since the novelty is detected first at level $\ell = 1$. Finally, notice that a branch such as $V_{1,1}^* \rightarrow V_{1,2}^* \rightarrow \text{“new”} \rightarrow V_{1,4}^*$ is not allowed in our representation. Under such a formulation, we are able to specify all the prior probabilities for both the observed taxa and the new ones in a coherent way.

B POSTERIOR TAXONOMIC PROBABILITIES

BayesANT assumes DNA sequences \mathbf{X}_i associated with leaf $v_L \in \mathcal{V}_L$ are distributed as

$$(\mathbf{X}_i \mid V_{i,L} = v_L, \boldsymbol{\theta}_{v_L}) \stackrel{\text{iid}}{\sim} \mathcal{K}(\mathbf{X}_i; \boldsymbol{\theta}_{v_L}),$$

where $\mathcal{K}(\cdot, \boldsymbol{\theta}_{v_L})$ is a distribution that depends on the leaf-specific vector of parameters $\boldsymbol{\theta}_{v_L}$. In what follows, we provide mathematical details of the single location product-multinomial model we use in the main document. Adapting the details to accommodate alternative kernels is straightforward.

B.1 MULTINOMIAL KERNEL

Let \mathbf{X}_i , $i = 1, \dots, n$, indicate a collection of *aligned* DNA sequences of length p . The alignment of the sequences makes the individual loci comparable across taxa. An example for $p = 20$ loci is as follows:

LOCUS s	1	2	3	4	5	6	7	8	9	10	11	12	13	14	15	16	17	18	19	20
\mathbf{X}_1 :	A	C	C	T	C	G	G	A	A	A	T	T	T	G	G	A	A	T	C	A
\mathbf{X}_2 :	A	C	T	T	C	G	A	A	T	A	T	A	A	G	A	G	A	T	G	G
\mathbf{X}_3 :	A	T	T	C	C	G	T	A	G	G	T	T	T	G	A	G	T	T	G	A

As each loci in each sequence corresponds to a nucleotide in $\mathcal{N}_1 = \{A, C, G, T\}$, it is natural to use a multinomial likelihood,

$$(X_{i,s} \mid V_{i,L} = v, \boldsymbol{\theta}_{v,s}) \stackrel{\text{iid}}{\sim} \text{MULT}(1; \theta_{v,s,A}, \theta_{v,s,C}, \theta_{v,s,G}, \theta_{v,s,T}),$$

where $\boldsymbol{\theta}_{v,s} = (\theta_{v,s,A}, \theta_{v,s,C}, \theta_{v,s,G}, \theta_{v,s,T})^\top$ is a vector of probabilities summing up to 1, and $\theta_{v,s,g}$ is the probability of observing nucleotide g in position s for leaf v . To simplify the analysis and ease computation, we further assume that all locations s are independent, leading to the following likelihood contribution for the i th sequence:

$$\mathcal{K}(\mathbf{X}_i; \boldsymbol{\theta}_v) = \prod_{s=1}^p \prod_{g \in \mathcal{N}_1} \theta_{v,s,g}^{\mathbf{1}\{X_{i,s}=g\}}, \quad (16)$$

where $\mathbf{1}\{\cdot\}$ denotes the indicator function. As a conjugate prior for the nucleotide probabilities, we choose

$$\boldsymbol{\theta}_{v,s} \sim \text{DIRICHLET}(\xi_{v,s,A}, \xi_{v,s,C}, \xi_{v,s,G}, \xi_{v,s,T}),$$

with $\boldsymbol{\xi}_{v,s} = (\xi_{v,s,A}, \xi_{v,s,C}, \xi_{v,s,G}, \xi_{v,s,T})^\top$ a vector of hyperparameters. The posterior distribution for the nucleotide probabilities at locus s under leaf v conditional on the DNA sequences assigned to v is then

$$(\boldsymbol{\theta}_{v,s} \mid \mathcal{D}_n) \sim \text{DIRICHLET}(\xi_{v,s,A} + n_{v,s,A}, \xi_{v,s,C} + n_{v,s,C}, \xi_{v,s,G} + n_{v,s,G}, \xi_{v,s,T} + n_{v,s,T}),$$

where $n_{v,s,g} = \sum_{i:V_{i,L}=v} \mathbf{1}\{X_{i,s} = g\}$ indicates the number of times nucleotide $g \in \mathcal{N}_1$ is recorded at locus s for the DNA sequences linked to leaf v . The resulting posterior kernel for $\boldsymbol{\theta}_v$ is then a product

of independent Dirichlet distributions, namely

$$p(\boldsymbol{\theta}_v | \mathcal{D}_n) \propto \prod_{s=1}^p \prod_{g \in \mathcal{N}_1} \theta_{v,s,g}^{\xi_{v,s,g} + n_{v,s,g}}. \quad (17)$$

An equivalent representation can be obtained for the 2-mer location multinomial kernel detailed in the main paper, but with the support of the multinomial being all pairs of nucleotides instead of singletons. When sequences are not aligned, the posterior in equation (17) is modified to remove the product from $s = 1, \dots, p$ and substitute $n_{v,s,g}$ with $n_{v,g}$, which is the number of times κ -mer g is recorded in the sequence.

B.2 PRIOR AND POSTERIOR PREDICTIVE DISTRIBUTION

Once the parameters for the posterior distribution in equation (17) have been computed for each leaf node v_L , BayesANT determines the prediction probabilities $p_{n+1}(v_L) = \text{pr}(V_{n+1,L} = v_L | \mathbf{X}_{n+1}, \mathcal{D}_n)$ as

$$p_{n+1}(v_L) \propto \pi_{n+1}(v_L) \int \mathcal{K}(\mathbf{X}_{n+1}; \boldsymbol{\theta}_{v_L}) p(\boldsymbol{\theta}_{v_L} | \mathcal{D}_n) d\boldsymbol{\theta}_{v_L}, \quad (18)$$

where $\pi_{n+1}(v_L)$ is the prior probability defined in equation (15), while the integral is the posterior predictive distribution for DNA sequence \mathbf{X}_{n+1} under leaf v_L . Notice that if v_L is a “new” taxon, equation (18) becomes a prior predictive distribution. For the multinomial kernel with Dirichlet prior defined above, the integral is explicitly available. Specifically, it is straightforward to see that the marginal distribution for $X_{i,s}$ when the posterior follows a Dirichlet is

$$X_{n+1,s} \sim \text{MULT}\left(1; \frac{\xi_{v,s,A} + n_{v,s,A}}{M_{v,s}}, \frac{\xi_{v,s,C} + n_{v,s,C}}{M_{v,s}}, \frac{\xi_{v,s,G} + n_{v,s,G}}{M_{v,s}}, \frac{\xi_{v,s,T} + n_{v,s,T}}{M_{v,s}}\right), \quad (19)$$

where $M_{v,s} = \sum_{g \in \mathcal{N}_1} (\xi_{v,s,g} + n_{v,s,g})$ is a normalizing constant for the nucleotide probabilities. The corresponding prior predictive probability is obtained by setting $n_{v,s,g} = 0$ for every $g \in \mathcal{N}_1$ and normalizing by $\xi_{v,s,0} = \sum_{g \in \mathcal{N}_1} \xi_{v,s,g}$. Then, from equation (19) and the location independence assumption, it can be easily shown that equation (18) reduces to

$$p_{n+1}(v_L) \propto \begin{cases} \pi_{n+1}(v_L) \prod_{s=1}^p (\xi_{v_L,s,g_s} + n_{v_L,s,g_s}) / M_{v_L,s}, & \text{if } v_L \text{ is an observed leaf,} \\ \pi_{n+1}(v_L) \prod_{s=1}^p \xi_{v_L,s,g_s} / \xi_{v,s,0}, & \text{if } v_L \text{ is a novel leaf,} \end{cases} \quad (20)$$

where $g_s \in \mathcal{N}_1$ is the nucleotide of sequence \mathbf{X}_{n+1} in locus $s = 1, \dots, p$. Similar considerations hold for both the κ -product multinomial kernel and for the not aligned multinomial kernel.

B.3 HYPERPARAMETER TUNING

From equation (20), it is straightforward to see that the hyperparameters $\xi_{v,s}$ play an important role in defining the prediction probabilities. This is especially true for “new” leaves, since no nucleotides are observed. As already discussed in the main paper, uniform priors in this context may underestimate the predicted number of new taxa at the lowest level. Therefore, we need a method to tune $\xi_{v,s}$ based on the information available in the taxonomic tree. To address this goal, we apply a method of moments estimator as detailed below.

For a node v_ℓ at level ℓ , call $\mathcal{L}_n(v_\ell)$ the set of leaves linked to it. Under the assumption that

$$\theta_{v,s} \stackrel{\text{iid}}{\sim} \text{DIRICHLET}(\xi_{v_\ell,s,A}, \xi_{v_\ell,s,C}, \xi_{v_\ell,s,G}, \xi_{v_\ell,s,T}), \quad \text{for all } v \in \mathcal{L}_n(v_\ell),$$

each nucleotide probability is marginally distributed as $\theta_{v,s,g} \sim \text{BETA}(\xi_{v_\ell,s,g}, \xi_{v_\ell,s,0} - \xi_{v_\ell,s,g})$, with $\xi_{v_\ell,s,0} = \sum_{g \in \mathcal{N}_1} \xi_{v_\ell,s,g}$ being the sum of the hyperparameters. From the moments of a beta distribution, it holds that

$$E[\theta_{v,s,g}] = \frac{\xi_{v_\ell,s,g}}{\xi_{v_\ell,s,0}}, \quad \text{and} \quad E[\theta_{v,s,g}^2] = \frac{\xi_{v_\ell,s,g}(\xi_{v_\ell,s,g} + 1)}{\xi_{v_\ell,s,0}(\xi_{v_\ell,s,0} + 1)},$$

for $g \in \mathcal{N}_1$. Our goal is to estimate both $\xi_{v_\ell,s,0}$ and $\xi_{v_\ell,s,g}$. This can be done as follows. Recall that $N_n(v)$ and $n_{v,s,g}$ are the number of sequences and the number of times nucleotide g is recorded at locus s for all sequences linked to leaf v , respectively. Our first method of the moments equation is

$$\hat{\theta}_{v_\ell,s,g} = \frac{1}{N_n(v_\ell)} \sum_{v \in \mathcal{L}_n(v_\ell)} \frac{n_{v,s,g}}{N_n(v)} = \frac{\xi_{v_\ell,s,g}}{\xi_{v_\ell,s,0}} = E[\theta_{v,s,g}]. \quad (21)$$

Here, $\hat{\theta}_{v_\ell,s,g}^g$ is an average of the observed proportion of times nucleotide g appears in the sequences linked to all leaves v connected to v_ℓ . For our second equation, we set

$$\hat{S}_{v_\ell,s} = \frac{1}{N_n(v_\ell)} \sum_{v \in \mathcal{L}_n(v_\ell)} \sum_{g \in \mathcal{N}_1} \left(\frac{n_{v,s,g}}{N_n(v)} \right)^2 = \sum_{g \in \mathcal{N}_1} \frac{\xi_{v_\ell,s,g}(\xi_{v_\ell,s,g} + 1)}{\xi_{v_\ell,s,0}(\xi_{v_\ell,s,0} + 1)} = \sum_{g \in \mathcal{N}_1} E[\theta_{v,s,g}^2], \quad (22)$$

where $\hat{S}_{v_\ell,s}$ is the average sum of the squared nucleotide proportions for all v linked to v_ℓ . Notice that the third component in the equation can be further simplified as

$$\sum_{g \in \mathcal{N}_1} E[\theta_{v,s,g}^2] = \sum_{g \in \mathcal{N}_1} \frac{\xi_{v_\ell,s,g}(\xi_{v_\ell,s,g} + 1)}{\xi_{v_\ell,s,0}(\xi_{v_\ell,s,0} + 1)} = \frac{1}{\xi_{v_\ell,s,0} + 1} \left\{ \xi_{v_\ell,s,0} \sum_{g \in \mathcal{N}_1} \left(\frac{\xi_{v_\ell,s,g}}{\xi_{v_\ell,s,0}} \right)^2 + 1 \right\}.$$

Then, plugging equation (21) into (22) and letting $m_{v_\ell,s} = \sum_{g \in \mathcal{N}_1} \hat{\theta}_{v_\ell,s,g}^2$, one has that

$$\hat{S}_{v_\ell,s} = \frac{1}{\xi_{v_\ell,s,0} + 1} (\xi_{v_\ell,s,0} m_{v_\ell,s} + 1),$$

which, combined with equation (21), yields

$$\xi_{v_\ell, s, 0} = \frac{1 - \hat{S}_{v_\ell, s}}{\hat{S}_{v_\ell, s} - m_{v_\ell, s}}, \quad \text{and} \quad \xi_{v_\ell, s, g} = \xi_{v_\ell, s, 0} \hat{\theta}_{v_\ell, s, g}, \quad g \in \mathcal{N}_1. \quad (23)$$

The quantities in equation (23) are the method of the moments estimators for our hyperparameters, and we can use them to borrow information across branches as discussed in the main paper. We detail the procedure in Algorithm 1 below.

Algorithm 1 Hyperparameter tuning via method of moments for the multinomial kernel

- 1: **for** leaf $v_L \in \mathcal{V}_L$ **do**
 - 2: **if** v_L is a *known* taxon **then**
 - 3: Estimate $\xi_{v_{L-1}, s, 0}$ and $\xi_{v_{L-1}, s, g}$, $g \in \mathcal{N}_1$, from equation (23), where $v_{L-1} = \text{pa}(v_L)$.
 - 4: Set prior $\boldsymbol{\theta}_{v_L, s} \sim \text{DIRICHLET}(\xi_{v_{L-1}, s, A}, \xi_{v_{L-1}, s, C}, \xi_{v_{L-1}, s, G}, \xi_{v_{L-1}, s, G})$
 - 5: **else if** v_L is a *new* taxon **then**
 - 6: Estimate $\xi_{v_\ell, s, 0}$ and $\xi_{v_\ell, s, g}$, $g \in \mathcal{N}_1$, from equation (23), where v_ℓ is the lowest possible *known* taxon along the branch leading to v_L
 - 7: Set prior $\boldsymbol{\theta}_{v_L, s} \sim \text{DIRICHLET}(\xi_{v_\ell, s, A}, \xi_{v_\ell, s, C}, \xi_{v_\ell, s, G}, \xi_{v_\ell, s, G})$
 - 8: **end if**
 - 9: **end for**
 - 10: Repeat procedure for all locations $s = 1, \dots, p$.
-

The idea behind Algorithm 1 is to incorporate taxonomic dependencies between the leaves, especially novel ones. The procedure works equally for the κ -product multinomial kernel.